



Cite this: DOI: 10.1039/d1cy00488c

Tetrathienoanthracene-functionalized conjugated microporous polymers as an efficient, metal-free visible-light solid organocatalyst for heterogeneous photocatalysis†

Chang-An Wang, * Jian-Ping Zhang, Kun Nie, Yan-Wei Li, Qun Li, Guo-Zheng Jiao, Jian-Guo Chang and Yin-Feng Han*

Owing to their advantages of superior inherent porosity, high chemical stability, light weight, and molecularly tunable optoelectronic properties, conjugated microporous polymers (CMPs) have been receiving increasing attention and research interest as promising alternatives to traditional inorganic semiconductors for heterogeneous photocatalysis. Herein, we report the concise synthesis of tetrathienoanthracene-based conjugated microporous polymers (TTA-CMP) *via* a bottom-up strategy. TTA-CMP was employed as metal-free visible-light solid organocatalyst for three prototypic organic reactions: the dehydrogenative coupling reaction, dehydrogenative-Mannich reaction, and photocatalytic synthesis of benzimidazoles. Indeed, TTA-CMP showed excellent photocatalytic activity (29 examples, 80–98% yield) and outstanding reusability (10–12 times) in these three reactions. The extended π -conjugation in TTA-CMP enhances its visible light absorption, therefore, TTA-CMP displays higher catalytic activity than the corresponding small molecular photocatalyst. This work reveals the bright future of TTA-CMP as an efficient solid organocatalyst for other photocatalytic syntheses.

Received 20th March 2021,
Accepted 20th April 2021

DOI: 10.1039/d1cy00488c

rsc.li/catalysis

Introduction

Organic photochemical synthesis *via* simulating the photosynthesis of natural plants has been the dream of synthetic chemists for more than 100 years.¹ In the past decade, since the pioneering work of MacMillan,² Yoon,³ and Stephenson,⁴ visible-light driven organic photochemical synthesis has undergone remarkable development.⁵ Because organic molecules lack the ability to absorb photons in the visible region, homogeneous photocatalysts such as $[\text{Ru}(\text{bpy})_3]^{2+}$ (bpy = 2,2'-bipyridine) and $[\text{Ir}(\text{ppy})_2(\text{bpy})]^+$ (ppy = 2-phenyl-pyridine) are often used to drive organic transformation due to their rich redox chemistry at the MLCT (metal-to-ligand charge-transfer) excited states.⁶ Indeed, in recent years, many photocatalytic reactions such as direct C–H functionalizations,⁷ the synthesis of aromatic aza-heterocycles,⁸ asymmetric photochemical reactions,^{2,9} and small molecule activation¹⁰ have been studied *via* different photoactivation modes. However, Ru and Ir metal ligands have intrinsic drawbacks, such as high toxicity, high price,

instability under aerobic conditions, and being difficult to remove after reactions, which impose a significant limit on large-scale synthesis.¹¹ From the viewpoints of industrial application and environmental friendliness, it is highly desirable to develop efficient photocatalytic solid organocatalysts with the advantages of being inexpensive, recyclable, and free of precious metals.¹² These solid organocatalysts can not only eliminate the contamination of organic products caused by heavy metal ions but can also reduce the processing costs in large-scale applications.¹³

Conjugated microporous polymers (CMPs),¹⁴ as one of the typical representatives of porous organic polymers (POPs) first reported by the Cooper group in 2007, have drawn considerable scientific attention due to their wide range of applications. CMPs have been widely used in the field of gas storage/separation,¹⁵ photoelectricity,¹⁶ chemosensors,¹⁷ and heterogeneous catalysis.¹⁸ Especially in recent years, CMP-based materials have garnered significant attention as promising candidates for photocatalytic applications.¹⁹ Compared with inorganic semiconductors, the outstanding features of π -conjugated polymers in the field of photocatalysis are:^{19d} (i) they consist of lightweight elements (C, H, O, N, S, *etc.*) with larger surface areas and they possess tunable energy levels for oxidation and reduction reactions; (ii) they can be easily prepared under mild conditions (less

College of Chemistry and Chemical Engineering, Taishan University, Tai'an, Shandong 271000, P. R. China. E-mail: wangcha@tsu.edu.cn, han@tsu.edu.cn

† Electronic supplementary information (ESI) available. See DOI: 10.1039/d1cy00488c

than 100 °C) and possess excellent chemical stability against photodecomposition; (iii) the skeleton structures of CMPs can be easily fine-tuned at the molecular level to better utilize visible light, while traditional inorganic photocatalysts can only use UV light; (iv) the extension of the π -conjugated structure of CMPs facilitates the separation of photogenerated charge carriers and their transport along the skeleton, which is crucial for driving photoredox reactions.

In this context, combining these features, here we report the design, synthesis, characterization, and photocatalytic performance of a new metal-free visible-light solid organocatalyst based on an anthra[1,2-*b*:4,3-*b'*:5,6-*b''*:8,7-*b'''*] tetrathioanthracene (TTA) core embedded CMP framework. Tetrathioanthracene (TTA) is a sulfur-rich polycyclic aromatic hydrocarbon with a flat and rigid π -conjugated structure, consisting of four thiophene units fused to an anthracene. It is well known that this structure tends to stack through strong π - π interactions and leads to excellent hole-carrier mobilities in organic field-effect transistors (OFETs).²⁰ Although functionalized tetrathioanthracene molecules are widely used in the synthesis of organic semiconductors *via* π - π stacking interactions,²¹ they are rarely used in the field of photocatalysis. Very recently, the An group²² and the Liu group²³ respectively reported the application of CMP materials based on similar structures of bithiophene and benzotrithiophene in heterogeneous photocatalysis. In this work, for the first time, we are incorporating tetrathioanthracene (TTA) into a three-dimensional π -conjugated microporous polymer framework (TTA-CMP), which could provide a heterogeneous photocatalytic system for visible light promoted organic transformations.

Results and discussion

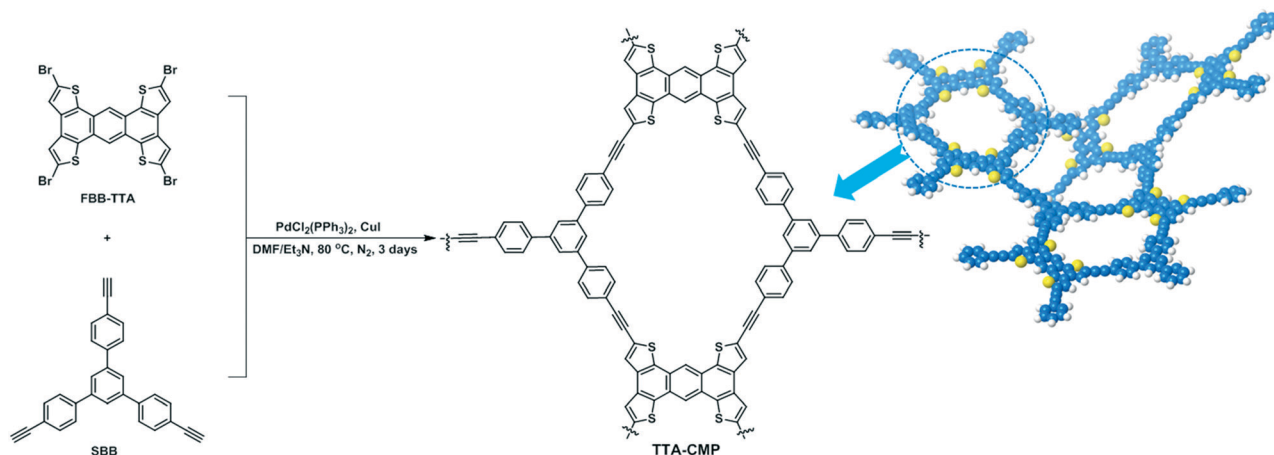
The designed synthesis and characterization of TTA-CMP

Tetrabromo-functionalized tetrathioanthracene was synthesized *via* a simple transformation from commercially available materials.^{20b} As shown in Scheme 1, we selected large-size 1,3,5-tri(4-ethynylphenyl)benzene as the structural building

block (denoted as SBB) and rigid, large-size, planar functionalized tetrathioanthracene as the functional building block (denoted as FBB-TTA). The TTA-CMP framework can be easily constructed in a high yield through the palladium catalyzed Sonogashira-Hagihara cross-coupling reaction under nitrogen atmosphere. The obtained polymeric framework is insoluble in water and general organic solvents such as MeOH, DMSO, DMF, THF, acetone and chloroform. It also retains high chemical stability even in acid or base solutions.

Further, the atomic-level linkages of the TTA-CMP framework were studied by using Fourier transform infrared (FT-IR) and ¹³C solid-state NMR spectroscopy. The FT-IR spectra of TTA-CMP and their monomers are exhibited in Fig. 1a. We found that the TTA-CMP polymer still retains many characteristic vibration signals of the TTA structure. Compared with the FT-IR spectrum of FBB-TTA and SBB, the absence of the C-H stretching peak of the -C≡C-H group around 3270 cm⁻¹ and the appearance of the characteristic peak at 2202 cm⁻¹ in the IR spectra of the TTA-CMP framework indicated the formation of a carbon-carbon triple-bond. Additionally, the FT-IR spectra for the TTA-CMP showed a strong peak for a thiophen ring at 820 cm⁻¹ (Fig. S1 in the ESI†). These results indicate that the polymerization process is efficient. The ¹³C solid-state NMR spectra of TTA-CMP exhibited signals at approximately 132, 128, 125, and 123 ppm, which originate from the carbon atoms of the tetrathioanthracene monomer. The signals at 142, 132, 125, and 121 ppm can be attributed to the carbon atoms of SBB, 1,3,5-tri(4-ethynylphenyl)benzene (the assignments are shown in Fig. 1b). The signals at 93 and 87 ppm are indicative of the formation of -C_{Ar}-C≡C-C_{heter}- sites. Additionally, the element analysis of the TTA-CMP framework confirmed the content of sulfur (10.95%) and the TTA photocatalyst loading could be calculated. All of these data provided overwhelming evidence that the functional monomer TTA was successfully embedded in the CMP skeleton.

The porosity of the TTA-CMP framework was tested by a nitrogen adsorption-desorption experiment at 77 K. As



Scheme 1 Synthesis of TTA-CMP *via* a bottom-up strategy.

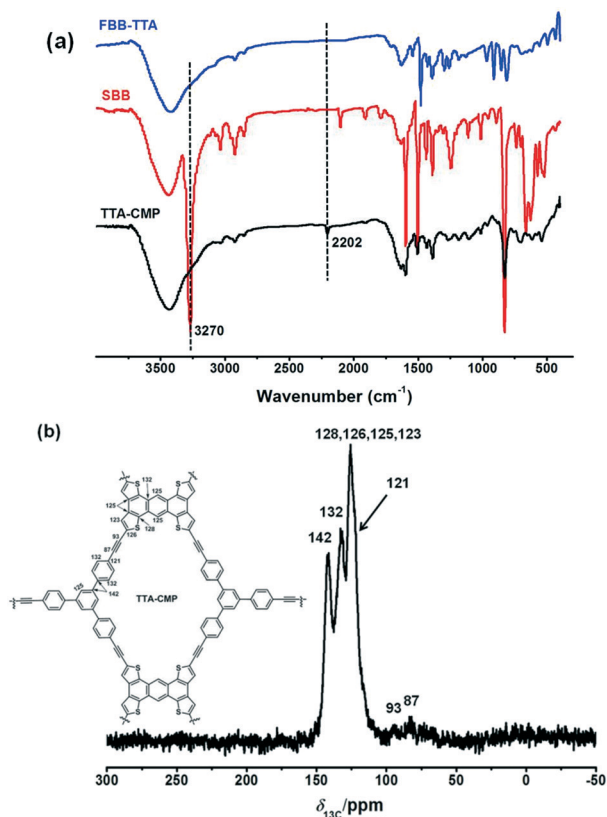


Fig. 1 (a) FT-IR spectra of FBB-TTA (blue line), SBB (red line) and TTA-CMP (black line). (b) The solid-state ^{13}C NMR spectrum of TTA-CMP and the assignments of ^{13}C chemical shifts of TTA-CMP are indicated in the chemical structure (left).

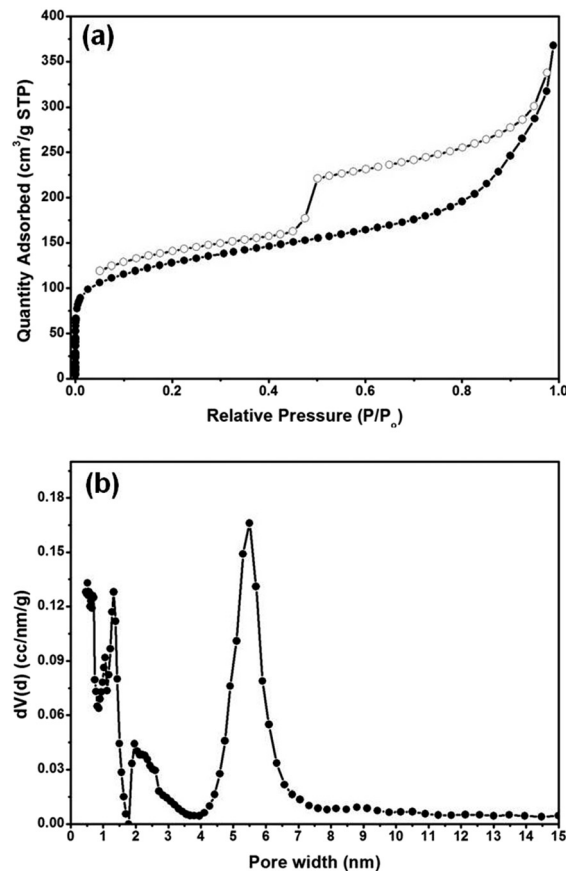


Fig. 2 (a) Nitrogen adsorption-desorption isotherms of TTA-CMP at 77 K. (b) The pore size distribution of TTA-CMP calculated by NL-DFT.

shown in Fig. 2a, TTA-CMP showed a type-IV sorption isotherm with H2 hysteresis loops, indicating that the TTA-CMP polymer displays mesoporous structures according to the IUPAC classification. Based on the nitrogen adsorption data, the Brunauer-Emmett-Teller (BET) surface area of TTA-CMP was calculated to be $461 \text{ m}^2 \text{ g}^{-1}$ and the total pore volume at $0.99P_0$ was evaluated to be $0.571 \text{ cm}^3 \text{ g}^{-1}$. Using the de Boer statistical thickness (t -plot) method, the TTA-CMP polymer displayed a micropore volume contribution of $0.105 \text{ cm}^3 \text{ g}^{-1}$ (18%) and a mesopore volume contribution of $0.466 \text{ cm}^3 \text{ g}^{-1}$ (82%). The pore-size distribution (PSD) was calculated by the nonlocal density functional theory (NL-DFT) model and was found to be centered at 1.3 nm, 2.2 nm and 5.5 nm, respectively (Fig. 2b). The PSD curves also demonstrated the existence of abundant mesopores in the TTA-CMP framework. For all we know, most of the currently reported catalytic POPs are microporous polymers (the pore size is less than 2 nm), the micropores are not conducive to mass transfer of the substrate molecule and the binding of the substrate to the catalytically active sites, this will reduce the catalytic activity of the porous catalysts. Therefore, the design and synthesis of CMP-based materials containing abundant mesopores is essential to improve the catalytic activity.²⁴

The TTA-CMP polymer is stable up to $300 \text{ }^\circ\text{C}$ in a nitrogen atmosphere (Fig. 3a), as revealed by thermogravimetric analysis (TGA). The SEM image indicates that the polymer consisted of bulk and spherical nanoparticles with a size of several hundred nanometers (Fig. 3b). The HR-TEM measurement displayed the presence of nanopores in the TTA-CMP network (Fig. 3c and S5[†]). In addition, energy-dispersive X-ray spectroscopy (EDX) elemental mapping images clearly showed that the elements C and S were homogeneously dispersed in the TTA-CMP network (Fig. 3d). The element analysis of TTA-CMP also confirmed the content of S and C in the networks. The PXRD analysis showed that TTA-CMP is an amorphous polymer, the same as our previously reported POP polymers^{13e,25} (Fig. S3 in the ESI[†]).

The optoelectronic properties of TTA-CMP were studied by solid-state UV/vis absorption spectroscopy and a cyclic voltammetry (CV) experiment. As shown in Fig. 4a, the TTA-CMP polymer exhibited a broad absorption region and the band edge extended to 800 nm. In comparison with the UV/vis absorption spectra of homogeneous FBB-TTA, the large range indicated that the extended-conjugation structure of TTA-CMP indeed enhances the visible light absorption region. The optical band gap (E_g) of TTA-CMP was 2.08 eV calculated by the Kubelka-Munk function (Fig. 4b). To evaluate the energy band structures of TTA-CMP, the cyclic

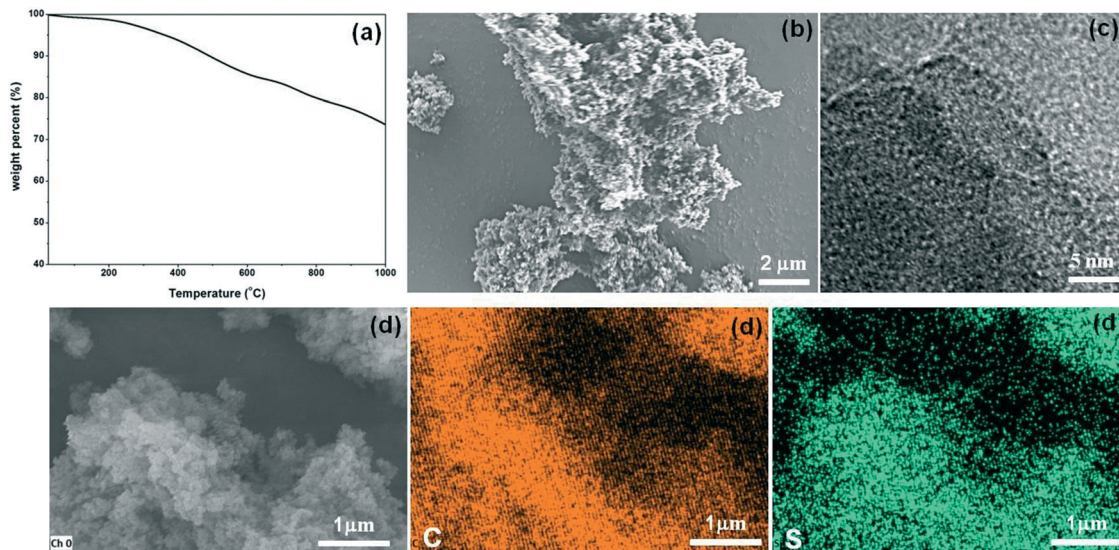


Fig. 3 (a) TGA curve of TTA-CMP. (b) SEM image of TTA-CMP. (c) HR-TEM image of TTA-CMP. (d) EDS mapping images of C and S for TTA-CMP.

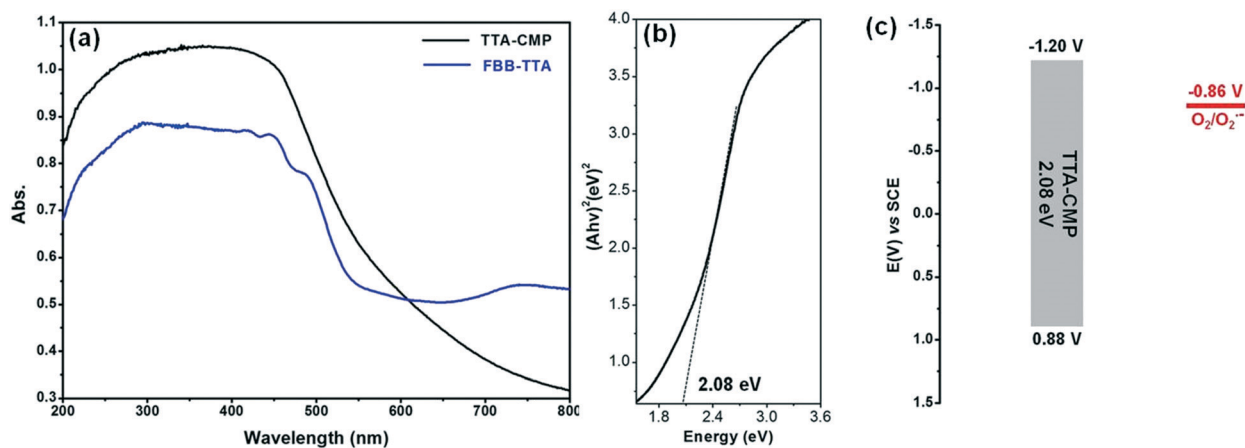


Fig. 4 (a) UV/vis absorption spectra of TTA-CMP (black) and the monomer (blue). (b) Kubelka-Munk plot (to measure the band gap energy) for solid-state TTA-CMP. (c) Energy band positions of the TTA-CMP and $O_2/O_2^{\cdot-}$ measured by CV.

voltammetry (CV) experiment was conducted (Fig. S6†). The conduction band position (E_c) of TTA-CMP versus SCE was at -1.20 V, the potential of the conduction band clearly indicates the reduction of O_2 to $O_2^{\cdot-}$ (-0.86 V vs. SCE), which was negative enough through photoinduced electron transfer from TTA-CMP to molecular O_2 under light illumination (Fig. 4c).

Photocatalytic application

The good photoredox properties, excellent stability, high BET surface and abundant mesopores of TTA-CMP ensured its excellent photocatalytic activity in visible-light driven organic transformations. Based on this, we selected three prototypic organic reactions to determine its photocatalytic activity, the scope of the substrates and the reusability of TTA-CMP were studied and the plausible mechanism of heterogeneous

photocatalytic reactions were proposed. We first chose the dehydrogenative coupling reaction of *N*-aryl-tetrahydroisoquinolines and nitroalkanes to examine the photocatalytic activity of the TTA-CMP polymer. The reaction of 2-phenyl-1,2,3,4-tetrahydroisoquinoline and nitromethane as a model reaction was first investigated to screen the conditions, and the results are shown in Table S1 in the ESI.† We found that TTA-CMP showed the best reactivity with 2.0 mol% catalyst loading in the presence of air with a common fluorescent lamp (24 W) as the light source at room temperature, giving the product in high yield (96%) after 12 h (Table S1,† entries 1–3). A number of control experiments were also conducted to demonstrate the photocatalytic nature of TTA-CMP. Natural light gave a low yield and the reaction did not work in the dark (Table S1,† entries 4–5), which indicated that light is necessary to promote the photoinduced electron transfer. The TTA-CMP polymer played a

heterogeneous catalytic role in the reaction, which was demonstrated by the background reaction in the absence of TTA-CMP (Table S1,† entry 6) and the non-photoactive CMP-1 as the heterogeneous catalyst (Table S1,† entry 7). In addition, O₂ played a critical role, which was demonstrated by the fact that the reaction proceeded much more slowly in nitrogen gas (Table S1,† entry 8). Importantly, it should be noted that the monomer FBB-TTA as the catalyst did not give a good yield (35%), implying that the extended π - π conjugated structure of CMP was advantageous for photocatalytic activity (Table S1,† entry 9). Under the established conditions, the substrate scope of the dehydrogenative coupling reaction catalyzed by TTA-CMP was examined. We evaluated the performance of different *N*-aryl-tetrahydroisoquinolines **1a–g** with nitroalkanes **2a–b** in the presence of 2.0 mol% TTA-CMP (Table 1). Both CH₃NO₂ (Table 1, **3a–3g**) and C₂H₅NO₂ (Table 1, **3h–3j**) as the nucleophile provided the desired products with good to excellent yields (90–98%). The results are comparable to those using the reported Ir- or Ru-loaded CMP,²⁶ RB-CMP,²⁷ EY-CMP,^{25a} and the homogeneous photocatalysts.^{7a,28} This demonstrates that the TTA-CMP framework can be used as an efficient heterogeneous organophotocatalyst for this class of dehydrogenative coupling reaction.

We next investigated the dehydrogenative-Mannich reaction²⁹ occurring between a tertiary amine and a ketone catalyzed by TTA-CMP. Whereas the TTA-CMP was once again shown to be a good photocatalyst for the oxidation of tertiary amine to generate the iminium ions *in situ* under light illumination, *L*-proline was used to generate the enamine nucleophiles from the ketone, which can easily react with the

iminium ions. In the dual catalytic Mannich-type reaction, we also evaluated the performance of different *N*-aryl-tetrahydroisoquinolines with the ketone in the presence of 2.0 mol% TTA-CMP and 20 mol% *L*-proline (Table 2). Various tetrahydroisoquinoline derivatives were reacted with acetone (Table 2, **5a–5g**) and butanone (Table 2, **5h–5j**) to provide the desired products in good to excellent yields (80–96%). To the best of our knowledge, the use of recyclable heterogeneous photocatalysts for dual-catalytic reactions has rarely been reported.^{13d,30}

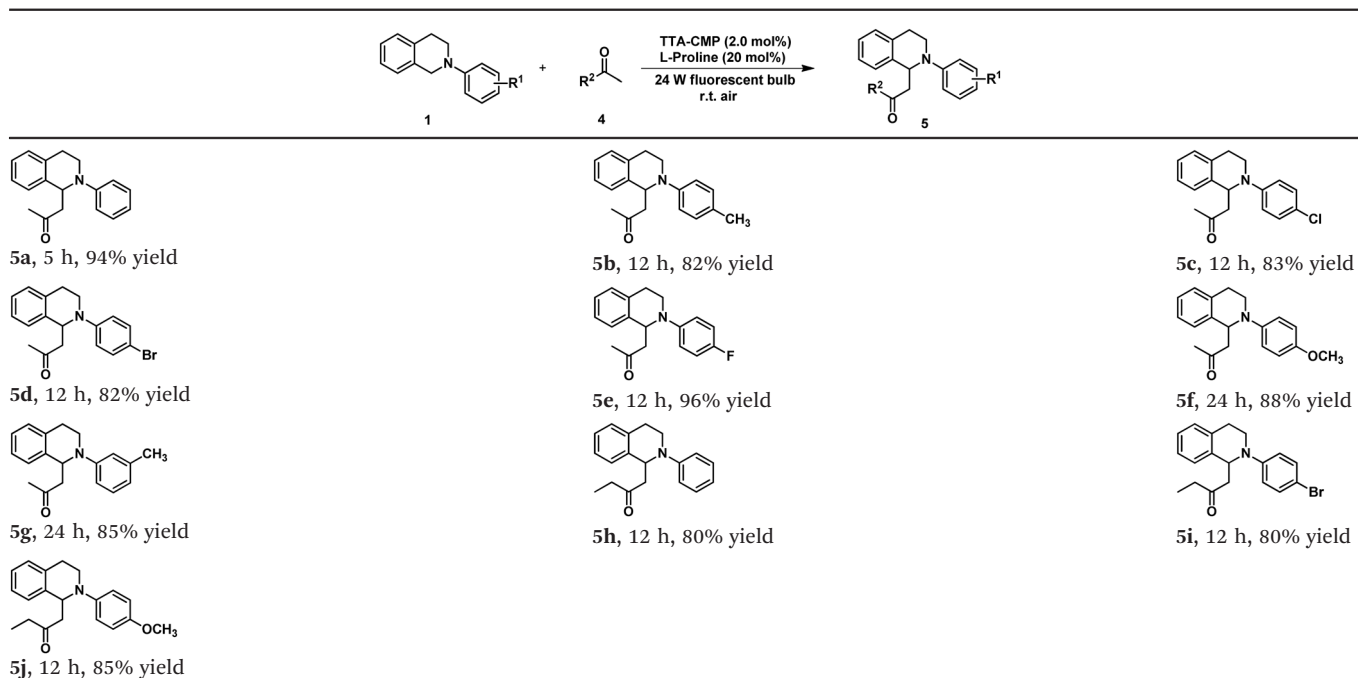
A possible reaction mechanism is proposed (Scheme 2). The excited state species TTA-CMP* is generated under visible light irradiation, which is reductively quenched by the tertiary amine **1** *via* a single electron transfer (SET) process to obtain a tertiary amine radical cation and a TTA-CMP^{•-} radical anion. The photoredox cycle is completed by the oxidation of TTA-CMP^{•-} back to the ground state TTA-CMP by molecular oxygen. The key intermediate iminium comes from the tertiary amine radical cation, which donates one hydrogen atom to the O₂^{•-}, it can be trapped by nucleophiles **2** or **4** under mild conditions to release the target product **3** or **5**. This plausible mechanism is also the most widely reported reaction mechanism in other groups.^{7a,28b}

The third reaction tested was the photocatalytic synthesis of benzimidazoles by TTA-CMP under visible light. The photosynthesis of 2-phenyl-benzimidazole as a model reaction was investigated to screen the conditions, and the results are shown in Table S2.† After screening the amount of catalyst and different solvents, we found that the use of 2.0 mol% TTA-CMP and ethanol as the solvent give the desired product in an excellent yield (see ESI,† Table S2, entries 1–11).

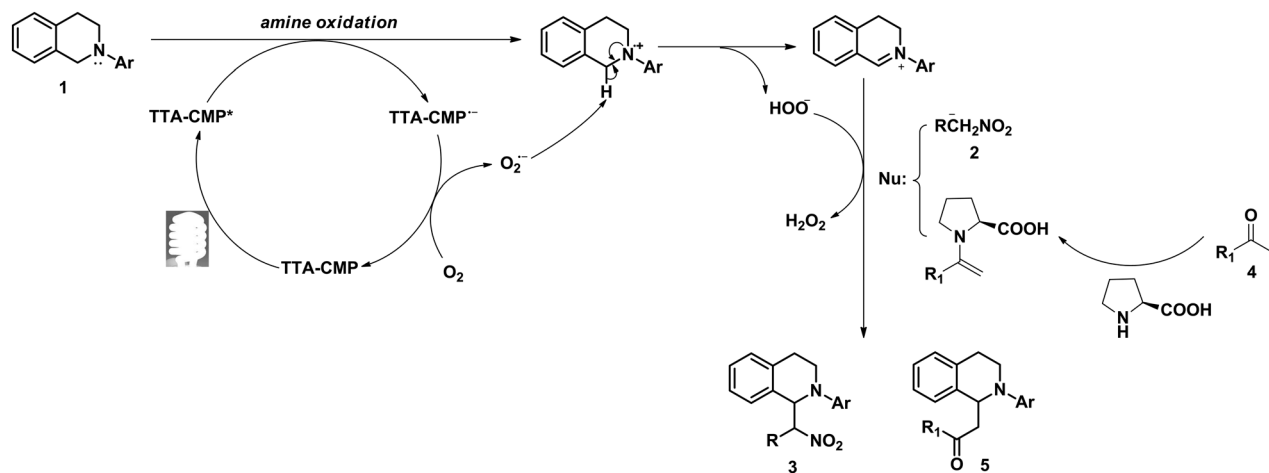
Table 1 Dehydrogenative coupling catalysed by TTA-CMP with visible light^a

 3a , 5 h, 96% yield	 3b , 12 h, 94% yield	 3c , 4 h, 96% yield
 3d , 5 h, 98% yield	 3e , 5 h, 94% yield	 3f , 24 h, 95% yield
 3g , 5 h, 90% yield	 3h , 5 h, 96% yield	 3i , 5 h, 92% yield
 3j , 5 h, 93% yield		

^a Reaction conditions: 0.2 mmol tertiary amine; 1.0 mL nitroalkane; TTA-CMP (4.7 mg, 2.0 mol%); room temperature; 24 W household bulb, in air. Isolated yields after silica gel column chromatography.

Table 2 Dehydrogenative-Mannich reaction catalysed by TTA-CMP under visible light^a

^a Reaction conditions: 0.1 mmol tertiary amine; 1.0 mL ketone; L-proline (2.3 mg, 20 mol%); TTA-CMP (2.4 mg, 2.0 mol%); room temperature; 24 W household bulb, in air. Isolated yields after silica gel column chromatography.

**Scheme 2** The proposed mechanism for TTA-CMP catalyzed dehydrogenative coupling.

Furthermore, some control experiments were carried out to determine whether visible light and the photocatalyst are necessary for the reaction (Table S2,† entries 12–16). The desired product was obtained in trace amounts or low yields when the reaction was performed in natural light, dark, and in the absence of TTA-CMP or the non-photoactive CMP-1 as the catalyst. It should also be noted that the monomer FBB-TTA as the catalyst did not give a good yield (72%), once again implying that the extended π - π conjugated structure of CMP was advantageous for photocatalytic activity (Table S1,† entry 17). Again, molecular O₂ played a critical role in the reaction (Table S1,† entry 18). The optimized reaction

conditions were determined as: 2.0 mol% TTA-CMP as the photocatalyst, ethanol as the solvent, irradiation with a 24 W blue bulb at ambient temperature in air. With the optimal photocatalytic conditions in hand, we next investigated the substrate scope of different aldehydes for the photocatalytic reaction catalyzed by the TTA-CMP polymer. As shown in Table 3, all the substrates of the aromatic aldehydes with different substituent groups, including benzaldehyde possessed -Br, -OH, -NO₂, -CN in the *p*-position (**8a–8e**), -Cl in the *o*-position (**8h**) and -CH₃ in the *m*-position (**8i**), 2-naphthaldehyde (**8f**), and 1-naphthaldehyde (**8g**), could furnish the corresponding benzimidazole derivatives

Table 3 Photocatalytic synthesis of benzimidazoles by TTA-CMP under visible light^a

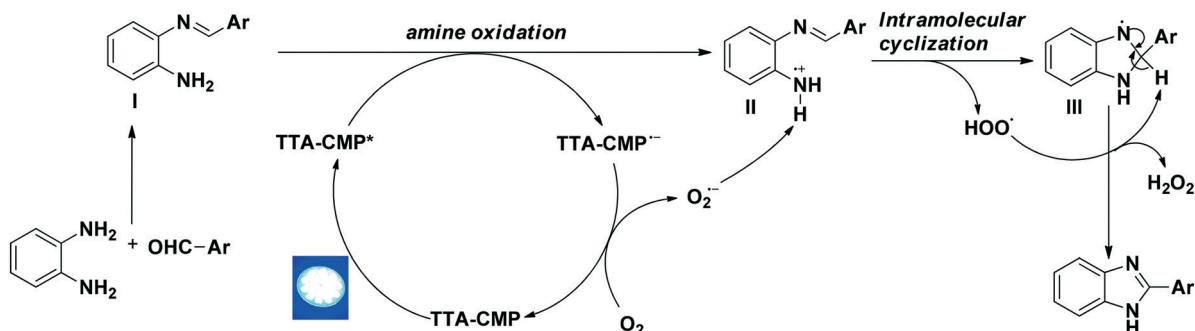
 8a , 2 h, 98% yield	 8b , 3 h, 98% yield	 8c , 8 h, 90% yield
 8d , 5 h, 83% yield	 8e , 5 h, 88% yield	 8f , 4 h, 94% yield
 8g , 5.5 h, 98% yield	 8h , 9 h, 87% yield	 8i , 6 h, 91% yield

^a Reaction conditions: 1,2-phenylenediamine (0.25 mmol), benzaldehyde (0.25 mmol), EtOH (3.0 mL), TTA-CMP catalyst (5.8 mg, 2.0 mol%), irradiation with 24 W blue bulb, room temperature, in air. Isolated yields after silica gel column chromatography.

smoothly in 2–9 h with good to excellent yields (Table 3, 83–98%). The geometries of the reactants and product of this photocatalytic reaction were optimized with the Gaussian 09 package at the B3LYP/6-31G(d) level in combination with frequency calculations (Fig. S8 in the ESI[†]). The three-dimensional sizes of 1,2-phenylenediamine, benzaldehyde and 2-phenylbenzimidazole were estimated to be 7.8 Å × 7.4 Å × 2.5 Å, 8.5 Å × 6.7 Å × 2.4 Å, and 13.3 Å × 7.4 Å × 2.4 Å, compared with the pore-size distribution (~5.5 nm) of TTA-CMP, it was clearly demonstrated that the reactants and product can be freely transported in the nanopores. Based on the synthesis of benzimidazoles catalyzed by other reported photocatalytic CMPs^{22,23} and the homogeneous photocatalysts,^{31,32} a possible reaction mechanism is proposed in Scheme 3. First, the excited state species TTA-CMP* is generated under visible light irradiation, which is reductively quenched by intermediate **I** *via* a single electron transfer (SET) process to obtain the intermediate **II** radical cation and the TTA-CMP^{•-} radical anion. The photoredox cycle is completed by the oxidation of TTA-CMP^{•-} back to the ground state TTA-CMP by molecular oxygen, and in this process O₂^{•-} is produced. The intermediate **II** radical cation donates one hydrogen proton to O₂^{•-} and then intermediate **III** is generated *via* intramolecular cyclization. Finally, after

losing hydrogen peroxide (Fig. S14 in the ESI[†]), the target product was obtained through the dehydrogenation process of **III**.

Besides the excellent photocatalytic activity and substrate tolerance, the reusability of TTA-CMP and its stability after reuse were studied. First, the catalytic recyclability of TTA-CMP was assessed by examining the photocatalytic dehydrogenative coupling reaction of 2-phenyl-1,2,3,4-tetrahydroisoquinoline and nitromethane (see ESI[†], Table S4), the photocatalytic dehydrogenative-Mannich reaction of 2-phenyl-1,2,3,4-tetrahydroisoquinoline and acetone (Table S5[†]) and the photocatalytic synthesis of 2-substituted benzimidazole of 1,2-phenylenediamine and benzaldehyde (Table S6[†]). After each cycle, the TTA-CMP polymer can be easily separated from the reaction solution by centrifugation. As shown in Fig. 5, no sign of significantly decreasing reactivity was observed after reusing TTA-CMP 10 times for the dehydrogenative coupling reaction (92–96%) and dehydrogenative-Mannich reaction (89–94%) and 12 times for the third reaction (92–98%). Second, after 12 cycles, the FT-IR spectra (see ESI[†], Fig. S10), UV-visible spectra (Fig. S11[†]), SEM (Fig. S12[†]), and EDX elemental mapping (Fig. S13[†]) of the recovered TTA-CMP indicate no apparent change in the skeleton structure. The BET surface area of TTA-CMP

**Scheme 3** The proposed mechanism for the photocatalytic synthesis of benzimidazole catalyzed by TTA-CMP under visible light.

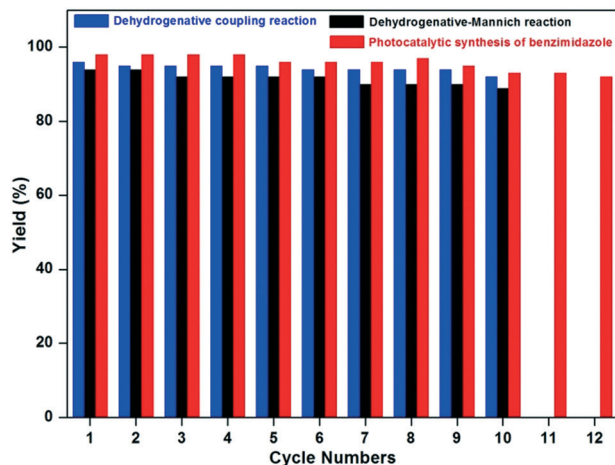
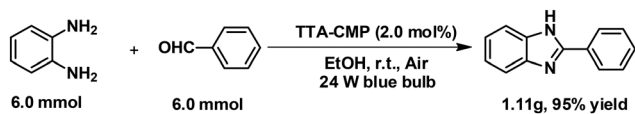


Fig. 5 Reusability of TTA-CMP in the photocatalyzed dehydrogenative coupling reaction of 2-phenyl-1,2,3,4-tetrahydroisoquinoline and nitromethane (blue), the dehydrogenative-Mannich reaction of 2-phenyl-1,2,3,4-tetrahydroisoquinoline and acetone (black), and the synthesis of 2-substituted benzimidazole of 1,2-phenylenediamine and benzaldehyde (red).



Scheme 4 The gram-scale photocatalytic synthesis of 2-phenyl-1H-benzimidazole.

decreased to $159 \text{ m}^2 \text{ g}^{-1}$ after the 10th recycled used, possibly due to the substrates or the products blocking the partial micropores of TTA-CMP (Fig. S9[†]). Pleasingly, as shown in Scheme 4, a gram scale experiment was carried out under optimal conditions without difficulty, attesting to the practicality of TTA-CMP in industry (Fig. S7[†]).

Conclusions

In summary, we used a bottom-up strategy to construct a metal-free solid porous organo-photocatalyst (TTA-CMP) for robust heterogeneous photocatalysis. Thanks to its excellent photoelectric properties, high BET surface area, mesoporous structure, and outstanding stability, the synthesized TTA-CMP was shown to be a highly active, recyclable and reusable heterogeneous photocatalyst in three different types of photoreactions. Compared with the photocatalytic activity of the monomer molecule, the unique extended π - π conjugation of the CMP materials is very important for improving the catalytic efficiency. Now, the exploration of CMP-based photocatalysts in asymmetric reactions is underway in our laboratory.

Conflicts of interest

There are no conflicts to declare.

Acknowledgements

This work was supported by the National Natural Science Foundation of China (No. 21502136 and 81803835) and the Shandong Outstanding Youth Innovation Team Program (No. 2019KJC032).

Notes and references

- Y. Chen, L.-Q. Lu, D.-G. Yu, C.-J. Zhu and W.-J. Xiao, Visible light-driven organic photochemical synthesis in China, *Sci. China: Chem.*, 2019, **62**, 24.
- D. A. Nicewicz and D. W. MacMillan, Merging photoredox catalysis with organocatalysis: the direct asymmetric alkylation of aldehydes, *Science*, 2008, **322**, 77.
- M. A. Ischay, M. E. Anzovino, J. Du and T. P. Yoon, Efficient Visible Light Photocatalysis of [2+2] Enone Cycloadditions, *J. Am. Chem. Soc.*, 2008, **130**, 12886.
- J. M. R. Narayanam, J. W. Tucker and C. R. J. Stephenson, Electron-Transfer Photoredox Catalysis: Development of a Tin-Free Reductive Dehalogenation Reaction, *J. Am. Chem. Soc.*, 2009, **131**, 8756.
- (a) M. D. Kärkäs, J. A. Porco and C. R. J. Stephenson, Photochemical Approaches to Complex Chemotypes: Applications in Natural Product Synthesis, *Chem. Rev.*, 2016, **116**, 9683; (b) D. Ravelli, S. Protti and M. Fagnoni, Carbon-Carbon Bond Forming Reactions via Photogenerated Intermediates, *Chem. Rev.*, 2016, **116**, 9850; (c) Q.-Q. Zhou, Y.-Q. Zou, L.-Q. Lu and W.-J. Xiao, Visible-Light-Induced Organic Photochemical Reactions through Energy-Transfer Pathways, *Angew. Chem., Int. Ed.*, 2019, **58**, 1586.
- (a) C. R. Bock, T. J. Meyer and D. G. Whitten, Electron transfer quenching of the luminescent excited state of tris(2,2'-bipyridine)ruthenium(II). Flash photolysis relaxation technique for measuring the rates of very rapid electron transfer reactions, *J. Am. Chem. Soc.*, 1974, **96**, 4710; (b) C. R. Bock, J. A. Connor, A. R. Gutierrez, T. J. Meyer, D. G. Whitten, B. P. Sullivan and J. K. Nagle, Estimation of excited-state redox potentials by electron-transfer quenching. Application of electron-transfer theory to excited-state redox processes, *J. Am. Chem. Soc.*, 1979, **101**, 4815.
- (a) A. G. Condie, J. C. Gonzalez-Gomez and C. R. Stephenson, Visible-light photoredox catalysis: aza-Henry reactions via C-H functionalization, *J. Am. Chem. Soc.*, 2010, **132**, 1464; (b) Y.-Q. Zou, L.-Q. Lu, L. Fu, N.-J. Chang, J. Rong, J.-R. Chen and W.-J. Xiao, Visible-Light-Induced Oxidation/[3+2] Cycloaddition/Oxidative Aromatization Sequence: A Photocatalytic Strategy To Construct Pyrrolo[2,1-a]isoquinolines, *Angew. Chem., Int. Ed.*, 2011, **50**, 7171; (c) J. Xie, Q. Xue, H. Jin, H. Li, Y. Cheng and C. Zhu, A visible-light-promoted aerobic C-H/C-N cleavage cascade to isoxazolidine skeletons, *Chem. Sci.*, 2013, **4**, 1281; (d) A. Hu, J.-J. Guo, H. Pan, H. Tang, Z. Gao and Z. Zuo, δ -Selective Functionalization of Alkanols Enabled by Visible-Light-Induced Ligand-to-Metal Charge Transfer, *J. Am. Chem. Soc.*, 2018, **140**, 1612.

- 8 (a) D. Zhao and Z. Xie, Visible-Light-Promoted Photocatalytic B–C Coupling via a Boron-Centered Carboranyl Radical: Facile Synthesis of B(3)-Arylated o-Carboranes, *Angew. Chem., Int. Ed.*, 2016, **55**, 3166; (b) G.-X. Li, C. A. Morales-Rivera, Y. Wang, F. Gao, G. He, P. Liu and G. Chen, Photoredox-mediated Minisci C–H alkylation of N-heteroarenes using boronic acids and hypervalent iodine, *Chem. Sci.*, 2016, **7**, 6407; (c) Y.-Y. Liu, X.-Y. Yu, J.-R. Chen, M.-M. Qiao, X. Qi, D.-Q. Shi and W.-J. Xiao, Visible-Light-Driven Aza-ortho-quinone Methide Generation for the Synthesis of Indoles in a Multicomponent Reaction, *Angew. Chem., Int. Ed.*, 2017, **56**, 9527.
- 9 (a) Y. Zhu, L. Zhang and S. Luo, Asymmetric α -Photoalkylation of β -Ketocarboxyls by Primary Amine Catalysis: Facile Access to Acyclic All-Carbon Quaternary Stereocenters, *J. Am. Chem. Soc.*, 2014, **136**, 14642; (b) Y. Yin, Y. Dai, H. Jia, J. Li, L. Bu, B. Qiao, X. Zhao and Z. Jiang, Conjugate Addition–Enantioselective Protonation of N-Aryl Glycines to α -Branched 2-Vinylazaarenes via Cooperative Photoredox and Asymmetric Catalysis, *J. Am. Chem. Soc.*, 2018, **140**, 6083; (c) Z. Yang, H. Li, S. Li, M.-T. Zhang and S. Luo, A chiral ion-pair photoredox organocatalyst: enantioselective anti-Markovnikov hydroetherification of alkenols, *Org. Chem. Front.*, 2017, **4**, 1037.
- 10 (a) A. Hu, J.-J. Guo, H. Pan and Z. Zuo, Selective functionalization of methane, ethane, and higher alkanes by cerium photocatalysis, *Science*, 2018, **361**, 668; (b) M. Majek and A. Jacobi von Wangelin, Metal-Free Carbonylations by Photoredox Catalysis, *Angew. Chem., Int. Ed.*, 2015, **54**, 2270.
- 11 C. Dai, J. M. R. Narayanam and C. R. J. Stephenson, Visible-light-mediated conversion of alcohols to halides, *Nat. Chem.*, 2011, **3**, 140.
- 12 (a) H. Xu, J. Gao and D. Jiang, Stable, crystalline, porous, covalent organic frameworks as a platform for chiral organocatalysts, *Nat. Chem.*, 2015, **7**, 905; (b) X. Wang, X. Han, J. Zhang, X. Wu, Y. Liu and Y. Cui, Homochiral 2D Porous Covalent Organic Frameworks for Heterogeneous Asymmetric Catalysis, *J. Am. Chem. Soc.*, 2016, **138**, 12332; (c) R. Chen, J.-L. Shi, Y. Ma, G. Lin, X. Lang and C. Wang, Designed Synthesis of a 2D Porphyrin-Based sp² Carbon-Conjugated Covalent Organic Framework for Heterogeneous Photocatalysis, *Angew. Chem., Int. Ed.*, 2019, **58**, 6430; (d) P.-F. Wei, M.-Z. Qi, Z.-P. Wang, S.-Y. Ding, W. Yu, Q. Liu, L.-K. Wang, H.-Z. Wang, W.-K. An and W. Wang, Benzoxazole-Linked Ultrastable Covalent Organic Frameworks for Photocatalysis, *J. Am. Chem. Soc.*, 2018, **140**, 4623; (e) M. Liu, Q. Huang, S. Wang, Z. Li, B. Li, S. Jin and B. Tan, Crystalline Covalent Triazine Frameworks by In Situ Oxidation of Alcohols to Aldehyde Monomers, *Angew. Chem., Int. Ed.*, 2018, **57**, 11968; (f) R. Li, J. Byun, W. Huang, C. Ayed, L. Wang and K. A. I. Zhang, Poly(benzothiadiazoles) and Their Derivatives as Heterogeneous Photocatalysts for Visible-Light-Driven Chemical Transformations, *ACS Catal.*, 2018, **8**, 4735; (g) Y. Wei, W. Chen, X. Zhao, S. Ding, S. Han and L. Chen, Solid-state emissive cyanostilbene based conjugated microporous polymers via cost-effective Knoevenagel polycondensation, *Polym. Chem.*, 2016, **7**, 3983; (h) Y. Zhi, Z. Li, X. Feng, H. Xia, Y. Zhang, Z. Shi, Y. Mu and X. Liu, Covalent organic frameworks as metal-free heterogeneous photocatalysts for organic transformations, *J. Mater. Chem. A*, 2017, **5**, 22933; (i) Y. Zhao, H. Liu, C. Wu, Z. Zhang, Q. Pan, F. Hu, R. Wang, P. Li, X. Huang and Z. Li, Fully Conjugated Two-Dimensional sp²-Carbon Covalent Organic Frameworks as Artificial Photosystem I with High Efficiency, *Angew. Chem., Int. Ed.*, 2019, **58**, 5376; (j) L. Li, W.-y. Lo, Z. Cai, N. Zhang and L. Yu, Donor–Acceptor Porous Conjugated Polymers for Photocatalytic Hydrogen Production: The Importance of Acceptor Comonomer, *Macromolecules*, 2016, **49**, 6903.
- 13 (a) Z. J. Wang, S. Ghasimi, K. Landfester and K. A. I. Zhang, Bandgap Engineering of Conjugated Nanoporous Polybenzobisthiadiazoles via Copolymerization for Enhanced Photocatalytic 1,2,3,4-Tetrahydroquinoline Synthesis under Visible Light, *Adv. Synth. Catal.*, 2016, **358**, 2576; (b) W. Zhang, J. Tang, W. Yu, Q. Huang, Y. Fu, G. Kuang, C. Pan and G. Yu, Visible Light-Driven C-3 Functionalization of Indoles over Conjugated Microporous Polymers, *ACS Catal.*, 2018, **8**, 8084; (c) Q. Huang, L. Guo, N. Wang, X. Zhu, S. Jin and B. Tan, Layered Thiazolo[5,4-d] Thiazole-Linked Conjugated Microporous Polymers with Heteroatom Adoption for Efficient Photocatalysis Application, *ACS Appl. Mater. Interfaces*, 2019, **11**, 15861; (d) J. Luo, X. Zhang and J. Zhang, Carbazolic Porous Organic Framework as an Efficient, Metal-Free Visible-Light Photocatalyst for Organic Synthesis, *ACS Catal.*, 2015, **5**, 2250; (e) C.-A. Wang, Y.-W. Li, Y.-F. Han, J.-P. Zhang, R.-T. Wu and G.-F. He, The “bottom-up” construction of chiral porous organic polymers for heterogeneous asymmetric organocatalysis: MacMillan catalyst built-in nanoporous organic frameworks, *Polym. Chem.*, 2017, **8**, 5561; (f) W. Liu, Q. Su, P. Ju, B. Guo, H. Zhou, G. Li and Q. Wu, A Hydrazone-Based Covalent Organic Framework as an Efficient and Reusable Photocatalyst for the Cross-Dehydrogenative Coupling Reaction of N-Aryltetrahydroisoquinolines, *ChemSusChem*, 2017, **10**, 664; (g) Z. J. Wang, K. Landfester and K. A. I. Zhang, Hierarchically porous π -conjugated polyHIPE as a heterogeneous photoinitiator for free radical polymerization under visible light, *Polym. Chem.*, 2014, **5**, 3559; (h) R. K. Yadav, A. Kumar, N.-J. Park, K.-J. Kong and J.-O. Baeg, A highly efficient covalent organic framework film photocatalyst for selective solar fuel production from CO₂, *J. Mater. Chem. A*, 2016, **4**, 9413; (i) X. Yan, H. Liu, Y. Li, W. Chen, T. Zhang, Z. Zhao, G. Xing and L. Chen, Ultrastable Covalent Organic Frameworks via Self-Polycondensation of an A2B2 Monomer for Heterogeneous Photocatalysis, *Macromolecules*, 2019, **52**, 7977; (j) G.-B. Wang, S. Li, C.-X. Yan, F.-C. Zhu, Q.-Q. Lin, K.-H. Xie, Y. Geng and Y.-B. Dong, Covalent organic frameworks: emerging high-performance platforms for efficient photocatalytic applications, *J. Mater. Chem. A*, 2020, **8**, 6957; (k) H. Liu, C. Li, H. Li, Y. Ren, J. Chen, J. Tang and Q. Yang, Structural Engineering of Two-Dimensional Covalent Organic Frameworks for Visible-Light-

- Driven Organic Transformations, *ACS Appl. Mater. Interfaces*, 2020, **12**, 20354; (l) Y. Zhi, K. Li, H. Xia, M. Xue, Y. Mu and X. Liu, Robust porous organic polymers as efficient heterogeneous organo-photocatalysts for aerobic oxidation reactions, *J. Mater. Chem. A*, 2017, **5**, 8697.
- 14 (a) A. I. Cooper, Conjugated Microporous Polymers, *Adv. Mater.*, 2009, **21**, 1291; (b) J.-X. Jiang, F. Su, A. Trewin, C. D. Wood, H. Niu, J. T. A. Jones, Y. Z. Khimyak and A. I. Cooper, Synthetic Control of the Pore Dimension and Surface Area in Conjugated Microporous Polymer and Copolymer Networks, *J. Am. Chem. Soc.*, 2008, **130**, 7710; (c) J.-X. Jiang, F. Su, A. Trewin, C. D. Wood, N. L. Campbell, H. Niu, C. Dickinson, A. Y. Ganin, M. J. Rosseinsky, Y. Z. Khimyak and A. I. Cooper, Conjugated Microporous Poly(aryleneethynylene) Networks, *Angew. Chem., Int. Ed.*, 2007, **46**, 8574.
- 15 (a) Q. Chen, M. Luo, P. Hammershøj, D. Zhou, Y. Han, B. W. Laursen, C.-G. Yan and B.-H. Han, Microporous Polycarbazole with High Specific Surface Area for Gas Storage and Separation, *J. Am. Chem. Soc.*, 2012, **134**, 6084; (b) T. Ben, H. Ren, S. Ma, D. Cao, J. Lan, X. Jing, W. Wang, J. Xu, F. Deng, J. M. Simmons, S. Qiu and G. Zhu, Targeted Synthesis of a Porous Aromatic Framework with High Stability and Exceptionally High Surface Area, *Angew. Chem., Int. Ed.*, 2009, **48**, 9457.
- 16 (a) Y. Xu, L. Chen, Z. Guo, A. Nagai and D. Jiang, Light-Emitting Conjugated Polymers with Microporous Network Architecture: Interweaving Scaffold Promotes Electronic Conjugation, Facilitates Exciton Migration, and Improves Luminescence, *J. Am. Chem. Soc.*, 2011, **133**, 17622; (b) L. Chen, Y. Honsho, S. Seki and D. Jiang, Light-Harvesting Conjugated Microporous Polymers: Rapid and Highly Efficient Flow of Light Energy with a Porous Polyphenylene Framework as Antenna, *J. Am. Chem. Soc.*, 2010, **132**, 6742.
- 17 (a) S. Gu, J. Guo, Q. Huang, J. He, Y. Fu, G. Kuang, C. Pan and G. Yu, 1,3,5-Triazine-Based Microporous Polymers with Tunable Porosities for CO₂ Capture and Fluorescent Sensing, *Macromolecules*, 2017, **50**, 8512; (b) J. Dong, A. K. Tummanapelli, X. Li, S. Ying, H. Hirao and D. Zhao, Fluorescent Porous Organic Frameworks Containing Molecular Rotors for Size-Selective Recognition, *Chem. Mater.*, 2016, **28**, 7889.
- 18 (a) Y.-B. Zhou and Z.-P. Zhan, Conjugated Microporous Polymers for Heterogeneous Catalysis, *Chem. - Asian J.*, 2018, **13**, 9; (b) M. Rose, Nanoporous Polymers: Bridging the Gap between Molecular and Solid Catalysts?, *ChemCatChem*, 2014, **6**, 1166; (c) Y. Zhang and S. N. Riduan, Functional porous organic polymers for heterogeneous catalysis, *Chem. Soc. Rev.*, 2012, **41**, 2083; (d) P. Kaur, J. T. Hupp and S. T. Nguyen, Porous Organic Polymers in Catalysis: Opportunities and Challenges, *ACS Catal.*, 2011, **1**, 819.
- 19 (a) S. Luo, Z. Zeng, G. Zeng, Z. Liu, R. Xiao, P. Xu, H. Wang, D. Huang, Y. Liu, B. Shao, Q. Liang, D. Wang, Q. He, L. Qin and Y. Fu, Recent advances in conjugated microporous polymers for photocatalysis: designs, applications, and prospects, *J. Mater. Chem. A*, 2020, **8**, 6434; (b) T. Zhang, G. Xing, W. Chen and L. Chen, Porous organic polymers: a promising platform for efficient photocatalysis, *Mater. Chem. Front.*, 2020, **4**, 332; (c) T.-X. Wang, H.-P. Liang, D. A. Anito, X. Ding and B.-H. Han, Emerging applications of porous organic polymers in visible-light photocatalysis, *J. Mater. Chem. A*, 2020, **8**, 7003; (d) C. Dai and B. Liu, Conjugated polymers for visible-light-driven photocatalysis, *Energy Environ. Sci.*, 2020, **13**, 24; (e) J. Byun and K. A. I. Zhang, Designing conjugated porous polymers for visible light-driven photocatalytic chemical transformations, *Mater. Horiz.*, 2020, **7**, 15.
- 20 (a) W.-J. Liu, Y. Zhou, Y. Ma, Y. Cao, J. Wang and J. Pei, Thin Film Organic Transistors from Air-Stable Heteroarenes: Anthra[1,2-b:4,3-b':5,6-b'':8,7-b''']tetrathiothiophene Derivatives, *Org. Lett.*, 2007, **9**, 4187; (b) J. L. Brusso, O. D. Hirst, A. Dadvand, S. Ganesan, F. Cicoira, C. M. Robertson, R. T. Oakley, F. Rosei and D. F. Perepichka, Two-Dimensional Structural Motif in Thienoacene Semiconductors: Synthesis, Structure, and Properties of Tetrathienoanthracene Isomers, *Chem. Mater.*, 2008, **20**, 2484.
- 21 (a) I. Zimmermann, J. Urieta-Mora, P. Gratia, J. Aragó, G. Grancini, A. Molina-Ontoria, E. Ortí, N. Martín and M. K. Nazeeruddin, High-Efficiency Perovskite Solar Cells Using Molecularly Engineered, Thiophene-Rich, Hole-Transporting Materials: Influence of Alkyl Chain Length on Power Conversion Efficiency, *Adv. Energy Mater.*, 2017, **7**, 1601674; (b) A. A. Leitch, A. Mansour, K. A. Stobo, I. Korobkov and J. L. Brusso, Functionalized Tetrathienoanthracene: Enhancing π - π Interactions Through Expansion of the π -Conjugated Framework, *Cryst. Growth Des.*, 2012, **12**, 1416.
- 22 W.-K. An, S.-J. Zheng, Y.-N. Du, S.-Y. Ding, Z.-J. Li, S. Jiang, Y. Qin, X. Liu, P.-F. Wei, Z.-Q. Cao, M. Song and Z. Pan, Thiophene-embedded conjugated microporous polymers for photocatalysis, *Catal. Sci. Technol.*, 2020, **10**, 5171.
- 23 S. Han, Z. Li, S. Ma, Y. Zhi, H. Xia, X. Chen and X. Liu, Bandgap engineering in benzotrithiophene-based conjugated microporous polymers: a strategy for screening metal-free heterogeneous photocatalysts, *J. Mater. Chem. A*, 2021, **9**, 3333.
- 24 (a) L.-P. Jing, J.-S. Sun, F. Sun, P. Chen and G. Zhu, Porous aromatic framework with mesopores as a platform for a super-efficient heterogeneous Pd-based organometallic catalysis, *Chem. Sci.*, 2018, **9**, 3523; (b) C.-A. Wang, Y.-F. Han, K. Nie and Y.-W. Li, Porous organic frameworks with mesopores and [Ru(bpy)₃]²⁺ ligand built-in as a highly efficient visible-light heterogeneous photocatalyst, *Mater. Chem. Front.*, 2019, **3**, 1909.
- 25 (a) C.-A. Wang, Y.-W. Li, X.-L. Cheng, J.-P. Zhang and Y.-F. Han, Eosin Y dye-based porous organic polymers for highly efficient heterogeneous photocatalytic dehydrogenative coupling reaction, *RSC Adv.*, 2017, **7**, 408; (b) C.-A. Wang, Y.-W. Li, X.-M. Hou, Y.-F. Han, K. Nie and J.-P. Zhang, N-Heterocyclic Carbene-based Microporous Organic Polymer Supported Palladium Catalyst for Carbon-Carbon Coupling Reaction, *ChemistrySelect*, 2016, **1**, 1371; (c) C.-A. Wang, Y.-F. Han, Y.-W. Li, K. Nie, X.-L. Cheng and J.-P. Zhang, Bipyridyl palladium embedded porous organic polymer as highly

- efficient and reusable heterogeneous catalyst for Suzuki-Miyaura coupling reaction, *RSC Adv.*, 2016, **6**, 34866.
- 26 (a) Z. Xie, C. Wang, K. E. deKrafft and W. Lin, Highly Stable and Porous Cross-Linked Polymers for Efficient Photocatalysis, *J. Am. Chem. Soc.*, 2011, **133**, 2056; (b) L. Pan, M.-Y. Xu, L.-J. Feng, Q. Chen, Y.-J. He and B.-H. Han, Conjugated microporous polycarbazole containing tris(2-phenylpyridine)iridium(iii) complexes: phosphorescence, porosity, and heterogeneous organic photocatalysis, *Polym. Chem.*, 2016, **7**, 2299.
- 27 J.-X. Jiang, Y. Li, X. Wu, J. Xiao, D. J. Adams and A. I. Cooper, Conjugated Microporous Polymers with Rose Bengal Dye for Highly Efficient Heterogeneous Organo-Photocatalysis, *Macromolecules*, 2013, **46**, 8779.
- 28 (a) Y. Pan, S. Wang, C. W. Kee, E. Dubuisson, Y. Yang, K. P. Loh and C.-H. Tan, Graphene oxide and Rose Bengal: oxidative C-H functionalisation of tertiary amines using visible light, *Green Chem.*, 2011, **13**, 3341; (b) Y. Pan, C. W. Kee, L. Chen and C.-H. Tan, Dehydrogenative coupling reactions catalysed by Rose Bengal using visible light irradiation, *Green Chem.*, 2011, **13**, 2682.
- 29 M. Rueping, C. Vila, R. M. Koenigs, K. Poschary and D. C. Fabry, Dual catalysis: combining photoredox and Lewis base catalysis for direct Mannich reactions, *Chem. Commun.*, 2011, **47**, 2360.
- 30 (a) L. Möhlmann, M. Baar, J. Rieß, M. Antonietti, X. Wang and S. Blechert, Carbon Nitride-Catalyzed Photoredox C-C Bond Formation with N-Aryltetrahydroisoquinolines, *Adv. Synth. Catal.*, 2012, **354**, 1909; (b) Y. Luo, Z.-Y. Xu, H. Wang, X.-W. Sun, Z.-T. Li and D.-W. Zhang, Porous Ru(bpy)₃²⁺-Linked Polymers for Recyclable Photocatalysis of Enantioselective Alkylation of Aldehydes, *ACS Macro Lett.*, 2020, **9**, 90.
- 31 S. Samanta, S. Das and P. Biswas, Photocatalysis by 3,6-Disubstituted-s-Tetrazine: Visible-Light Driven Metal-Free Green Synthesis of 2-Substituted Benzimidazole and Benzothiazole, *J. Org. Chem.*, 2013, **78**, 11184.
- 32 Z. Li, H. Song, R. Guo, M. Zuo, C. Hou, S. Sun, X. He, Z. Sun and W. Chu, Visible-light-induced condensation cyclization to synthesize benzimidazoles using fluorescein as a photocatalyst, *Green Chem.*, 2019, **21**, 3602.